SPECIAL PROJECT PROGRESS REPORT

All the following mandatory information needs to be provided. The length should *reflect the complexity and duration* of the project.

Reporting year	………………2023……………………………….……
Project Title:	Exploit observations to constrain land cover, vegetation and hydrology processes for improved near-term climate predictions over land
Computer Project Account:	………… spitales ……………………………….……
Principal Investigator(s):	……… Andrea Alessandri (Fransje van Oorschot, Emanuele Di Carlo, Annalisa Cherchi, Franco Catalano, Etienne Tourigny, Pablo Ortega)………………
Affiliation:	…… ISAC-CNR ……………………………….……
Name of ECMWF scientist(s) collaborating to the project (if applicable)	G. Balsamo (ECMWF), S. Boussetta, T. Stockdale and M. Balmaseda
Start date of the project:	………2022………………………………….……
Expected end date:	………2023……………………………………….……

Computer resources allocated/used for the current year and the previous one

(if applicable)

Please answer for all project resources

		Previous year		Current year	
		Allocated	Used	Allocated	Used
High Performance Computing Facility	(units)	24150000	25412885	11000000	15237
Data storage capacity	(Gbytes)	40000	9945	70000	10005

Summary of project objectives (10 lines max)

The objective of this special project is to exploit the latest available observational data over land to improve the representation of processes related to land cover, vegetation and hydrology that can positively contribute to skillful near-term climate predictions. Parameter-fitting and/or inverse modelling techniques will be employed to better constrain the land surface parameterizations to the available observations followed by careful verification that will be first conducted off-line through ERA-5 forced land-only simulations. Finally, a set of decadal predictions with enhanced representation of land cover, vegetation and hydrology processes will be performed to assess the improvement of the predictions.

Summary of problems encountered (10 lines max)

We experienced major problems in the porting of the decadal prediction system based on the version 3 of the EC-Earth ESM on the Atos machine, mainly due to difficulties in adapting the Autosubmit workflow manager. It followed the decision by the EC-Earth prediction WG to not port this old system anymore but to concentrate on the development of a new decadal prediction system based on EC-Earth4 (to be expected on Atos after 2024). Consequently, we performed as much as possible the decadal hindcast sensitivity (DCPP-VEG) before cca was switched off. To this aim in 2022 we requested additional resources (16150000 SBUs) for SPITALES.

Summary of plans for the continuation of the project (10 lines max)

In the remaining of this special project [note that an amendement has been submitted to special_projects@ecmwf.int to request that the remaining resources allocated for 2023 (11000000) are splitted into two years, i.e. 2023 (5000000) and 2024 (6000000)], we plan to investigate the feasibility of using an initialized dynamical vegetation model to interactively predict the land cover/vegetation evolution online during the simulations. The capability to simulate realistic vegetation variability will be first investigated by performing off-line simulations forced by ERA5 reanalysis and with the LPJ-Guess dynamical vegetation model turned on. After the preliminary off-line evaluation and depending on the off-line results, we'll consider to conduct historical simulations with a post-CMIP6 configuration of EC-Earth3 – that includes proper representation of the vegetation dynamics – to investigate the feasibility of actual forecasts with initialized vegetation.

List of publications/reports from the project with complete references

Di Carlo, E., Alessandri, A, van Oorschot, F., Catalano, F., Cherchi, A., and co-authors.: Effects of the realistic vegetation cover on predictions at decadal time scale. In preparation.

van Oorschot, F., van der Ent, R. J., Hrachowitz, M., Di Carlo, E., Catalano, F., Boussetta, S., Balsamo, G., and Alessandri, A.: Representing inter-annual land cover and vegetation variability based on satellite observations in the HTESSEL land surface model, EGUsphere [preprint], https://doi.org/10.5194/egusphere-2023-803, 2023

Summary of results

If submitted **during the first project year**, please summarise the results achieved during the period from the project start to June of the current year. A few paragraphs might be sufficient. If submitted **during the second project year**, this summary should be more detailed and cover the period from the project start. The length, at most 8 pages, should reflect the complexity of the project. Alternatively, it could be replaced by a short summary plus an existing scientific report on the project attached to this document. If submitted **during the third project year**, please summarise the results achieved during the period from July of the previous year to June of the current year. A few paragraphs might be sufficient.

1. Off-line land-only simulations forced by ERA-5

We evaluated the effects of integrating spatially and temporally varying land cover and vegetation characteristics derived from satellite observations on modelled evaporation and soil moisture in the Hydrology Tiled ECMWF Scheme for Surface Exchanges (HTESSEL; Balsamo et al., 2009) land surface model. Specifically, we integrated inter-annually varying land cover from the ESA-CCI (Copernicus Global Climate Change Service, 2022), and inter-annually varying Leaf Area Index (LAI) from the CGLS (Copernicus Global Land Service, 2022). Additionally, satellite data of the Fraction of green vegetation Cover (FCover) from CGLS was used to formulate and integrate a spatially and temporally varying effective vegetation cover parameterization. The overall effects of these three implementations on model evaporation fluxes and soil moisture were analysed using historical offline (land-only) model experiments at the global scale forced by ERA-5 (hereinafter SENS experiment). Model performances were quantified for evaporation by comparing with DOLCEv3 as reference data (Hobeichi et al., 2021) and for near-surface soil moisture by comparing with ESA-CCI SM as reference data (Dorigo et al., 2017; Gruber et al., 2019). The control experiment CTR uses temporally fixed land-cover from ESA-CCI for the year 1993, seasonal climatology of LAI based on CGLS for 1993-2019, and the effective vegetation cover parameterization with a spatially fixed shape of the relation between LAI and effective vegetation cover as used in EC-Earth3 (Doscher et al., 2022). In the SENS experiment we implemented annually varying land cover from ESA-CCI, inter-annually and seasonally varying LAI from CGLS, and the improved effective vegetation cover parameterization. More details on the model experiments can be found in Oorschot et al. (2023).

Correlation coefficients of evaporation and near surface soil moisture significantly improved with the improved vegetation and land cover representation (experiment SENS) compared to the CTR model-setup (Figure 1). Largest improvements were found in semi-arid regions, during the dry season (Figure 1). These improvements are related to the activation of soil moisture-evaporation feedbacks during vegetation-water-stressed periods with inter-annually varying LAI in combination with inter-annually varying effective vegetation cover, defined as an exponential function of LAI. More detailed results of the individual effects of three model implementations are presented in van Oorschot et al. (2023).

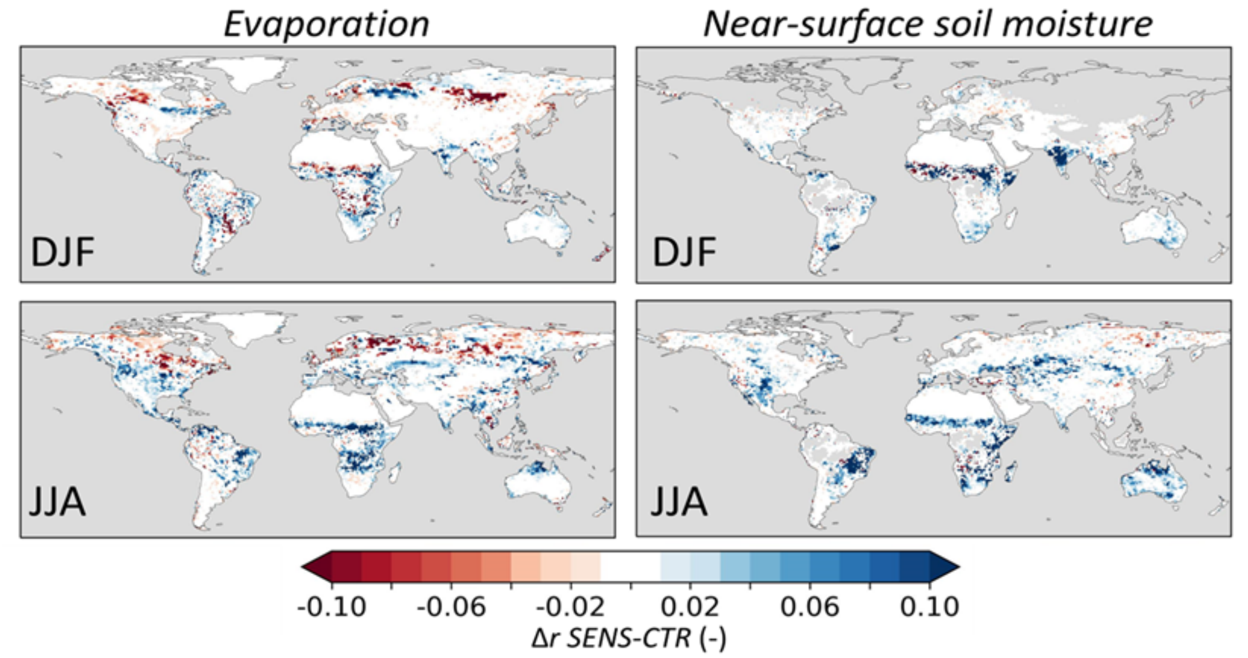

Fig 1. Pearson correlation coefficient difference (Δr) between experiment CTR and SENS (SENS–CTR) for (a,c) seasonal anomaly total evaporation with respect to DOLCEv3 evaporation for DJF and JJA and (b, d) seasonal anomaly near-surface soil moisture with respect to ESA-CCI SM for DJF and JJA. Blue (red) indicates an increased (reduced) correlation in SENS compared to CTR, white colors indicate small and/or insignificant Δr, and grey indicates no data points.

2. The decadal prediction experiment with the improved vegetation representation in the EC-Earth ESM

We performed a set of decadal sensitivity hindcasts (hereinafter referred to as DCPP-VEG) with the improved representation of vegetation variability (including the improved parameterization of the vegetation effective cover) based on the new satellite data as described in Van Oorschot et al., (2023; See Subsection 1 for a summary). In DCPP-VEG the interannual vegetation variability is prescribed from observations (LAI from CGLS-C3S and land cover from CGLS/ESA-CCI) therefore it is a potential predictability experiment, i.e., it is evaluated the best skill obtainable with perfect knowledge of the future state of vegetation.
This replaces the naïve representation of vegetation in the control decadal hindcasts already performed at BSC as their tier-1 (Component A1) contribution to the Decadal Climate Prediction Project (hereinafter DCPP-CTRL; Bilbao et al., 2021). In DCPP-CTRL, the LAI and Land Cover were prescribed as derived from a previous EC-Earth historical simulation that included an interactive dynamic of vegetation (first member of EC-Earth3-Veg contribution to historical simulation in CMP6) as provided by the on-line coupling with the Lund-Potsdam-Jena General Ecosystem Simulator (LPJ-GUESS; Smith et al., 2014).
The decadal hindcasts were performed with the EC-Earth version 3 atmosphere-ocean general circulation model in standard resolution (Döscher and the EC-Earth consortium., 2021). The atmospheric component is the Integrated Forecast System (IFS, cy36r4) from the European Centre for Medium-Range Weather Forecasts (ECMWF) that includes the HTESSEL land surface model as an integrated module. It has a T255 horizontal resolution (about 80km at the equator) and 91 vertical levels. The oceanic component is the Nucleus for European Modelling of the Ocean (NEMO; Madec and the NEMO Team; 2016). The ocean has a tripolar grid with a 1° horizontal resolution and 75 vertical levels (ORCA1). The atmospheric and ocean components are coupled through OASIS (Craig et al., 2017). The decadal experiment follows the CMIP6 DCPP-A protocol (Boer et al., 2017). It consists of 10 ensemble members of 5 years predictions initialized on the first of November of every year from 1993 to 2014.

The simulations have been performed using the semi-automated procedure based on the Autosubmit workflow manager (https://autosubmit.readthedocs.io/en/v3.13.0/). This was set up in collaboration with colleagues at Barcelona Supercomputing Centre (BSC) during the first year of the special project and adapted in order to perform parallel scheduling of the decadal predictions, preprocessing and post-processing.

DCPP-CTRL and DCPP-VEG share the same configuration, resolution, and Initial Conditions (ICs) for all components but the land surface (See Table 1 for a summary of the experimental setup). For both DCPP-VEG and DCPP-CTRL the atmospheric ICs are derived from ERA-Interim (Dee et al., 2011); oceanic ICs for temperature and salinity come from the ECMWF Ocean Reanalysis System 4 (ORAS4; Mogensen et al., 2012); both DCPP-VEG and DCPP-CTRL use prescribed radiative forcings from historical estimates for the period 1993-2014 and the CMIP6 SSP2-4.5 scenario for the period 2015-2019 (Eyring et al., 2016).
For the DCPP-VEG land ICs, a new ERA-Land-type offline simulation has been performed by prescribing the ERA5 (Hersbach et al., 2020) atmospheric forcing to the improved version of HTESSEL (Van Oorschot et al., 2023). This was needed to ensure consistency of the initialised land states with the novel HTESSEL developments in DCPP-VEG so that to avoid any possibility of artificial drifts that could affect the comparison. On the other hand, the land ICs for DCPP-CTRL were generated within DCPP (Component A1) with the original version of HTESSEL through an off-line ERA-Land simulation forced by the ERA-Interim reanalysis (Balsamo et al., 2015); in this case, the raw precipitation from ERA-Interim was bias-corrected to match the monthly climatology of the gridded observational product from the Global Precipitation Climatology Project [GPCP, Adler et al. (2018); see Bilbao et al (2021) for details about the bias correction procedure]. See Table 1 for a summary of the DCPP-CTRL and DCPP-VEG setups.

	DCPP-CTRL	**DCPP-VEG -potential predictability**
Period	1993-2014	1993-2014
Start Dates	1 November	1 November
Members\Lenght	10\5 years	10\5 years
Atmospheric IC	ERA-Interim	ERA-Interim
Ocean IC	ORAS4	ORAS4
LAI and Land Cover	prescribed and derived from an EC-Earth historical simulation coupled with the LPJ-GUESS	Prescribed interannually Varying LAI (CGLS-C3S) and land cover (CGLS/ESA-CCI)
Effective vegetation cover parameterization	prescribed and derived from an EC-Earth historical simulation coupled with the LPJ-GUESS	Effective cover parameterization as a function of LAI (K for each vegetation type)
Land IC	Offline ERA-Interim/Land type	Offline ERA5/Land type

Table 1: Experimental setup for DCPP-CTRL and DCPP-VEG.

To investigate the effects of the improved vegetation representation in DCPP-VEG, the forecasts at 3-year lead time, valid for the 4–5 year forecast period (i.e., the mean of the last two years in each forecast) are considered in all the analysis that follows. As reference data for the evaluation of the hindcast performance, we use the ERA5 dataset (Hersbach et al., 2020).

Figure 2 compares the biases in two-meter temperature. Panel a) reports the DCPP-CTRL bias, panel b) is the bias of DCPP-VEG, while panel c) shows the DCPP-VEG minus DCPP-CTRL bias difference. In panels a) and b) it is shown that the EC-Earth model, in general, tends to have a negative bias in the two-meter temperature when compared with ERA5. When considering the Boreal hemisphere, the cold bias has larger values over Sahara and the boreal forests, while positive values can be found only for three small regions in the east of the Caspian Sea, the east coasts of North America and Asia (the last two are regions characterized by intense baroclinicity and where the storm tracks are generated). The southern hemisphere shows quite a different behaviour; the bias over the continents tends to remain negative, but it becomes mostly positive over the Southern Oceans, especially at latitudes larger than 40S. The difference between the two experiments, Panel c), shows a general improvement of the bias and in particular over Siberia, Europe, Greenland, and tropical forests (South America, Africa and Southeast Asia). On the other hand, North American boreal forests and arid regions such as Sahara are an exception to the general bias improvement with an increase of the cold bias in DCPP-VEG. The Northern Hemisphere Oceans also show a bias improvement over North Atlantic, Labrador Sea, Hudson Bay, North Pacific Ocean, and Bering Sea with a small (0.1K - 0.5K) but statistically significant reduction of the temperature bias. These improvements are localized in a latitudinal band between 40N and 80N.

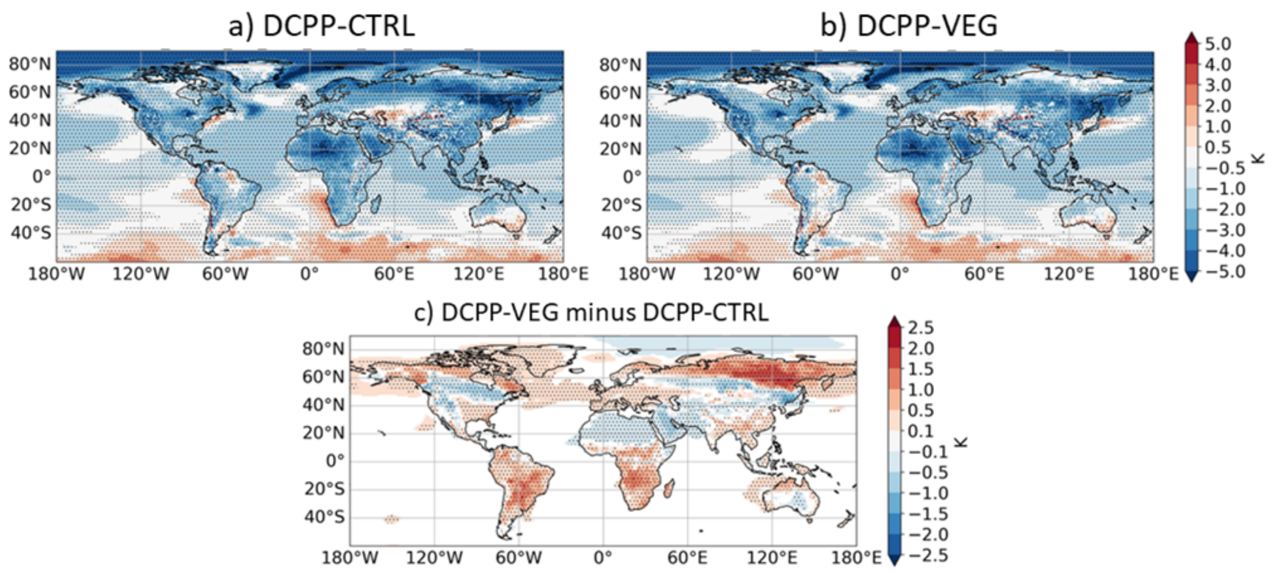

Fig 2: 2m temperature bias versus ERA5. a) DCPP-CTRL bias. b) DCPP-VEG bias. C) Bias difference, DCPP-VEG minus DCPP-CTRL. Dots represent statistically significant values, α=0.05.

The effect of the improved vegetation representation on the prediction skill measured in terms of the Anomaly correlation coefficient (ACC) is shown in Fig3. Panel a) shows the DCPP-CTRL ACC while panel b) is for the DCPP-VEG ACC. The model has a prediction skill characterized by a strong regionality; some regions have high ACC values, and others have almost no skill. Over the continents, the prediction skill is limited; regions with good skill are boreal hemisphere high latitudes (over 60N) except Greenland, Central Europe, Southwest of the United States, and North Africa. In contrast, the model prediction skill is low in central Asia, North America (between 40N and 60N), and Greenland; these are regions where ACC values are near zero or negative. When we focus on the oceans, the Mediterranean, the Indian Ocean and the Western Pacific Ocean

(in the summer Intertropical Convergence Zone) are the basins with the best ACC values. On the other hand, the North Atlantic shows low prediction skills.
When we compare the DCPP-VEG and DCPP-CTRL experiments (Fig. 2, Panel c), we see that the ACC improvement is confined to a few regions. The strongest signal is in central Asia in correspondence with the boreal forest. Another strong signal is over the Bering Sea and a third ACC improvement is over the deciduous forests in the southeast of the United States. The ACC improvement in central Asia is in a region where the DCPP-CTRL experiment has almost no skill and can be related to interannual variability in the land cover introduced with the model's improved vegetation. On the other hand, the potential predictability improvement over the Bering Sea cannot be associated with changes in land cover, but is most likely related to remote effects due to changes in the nearby land masses.

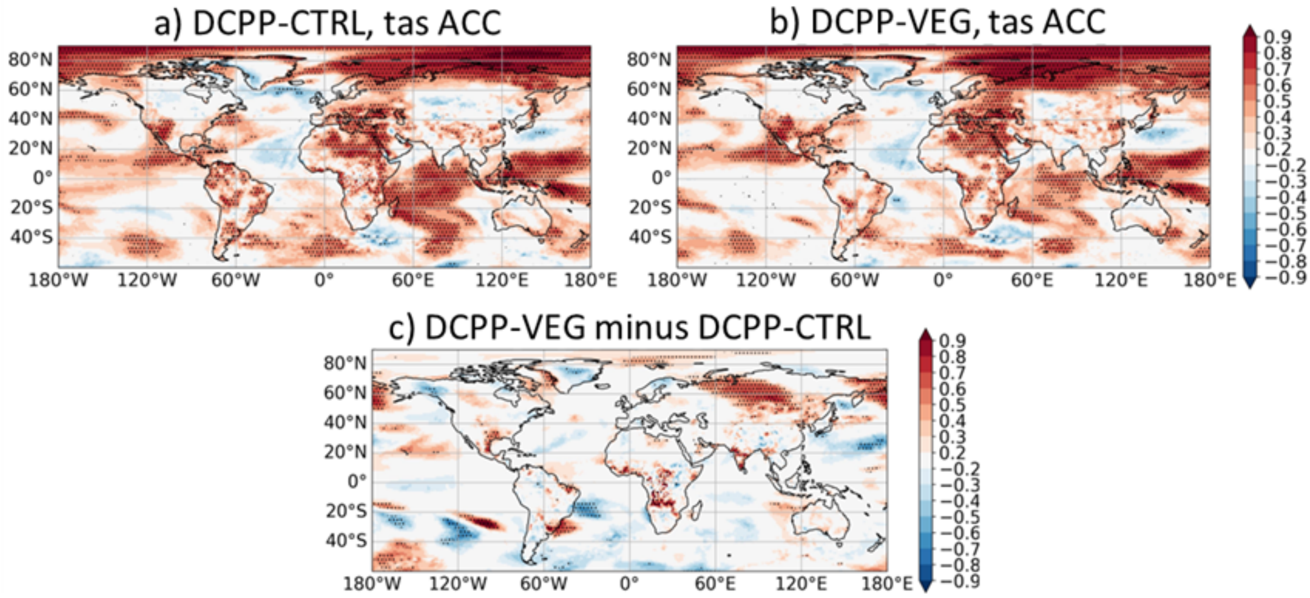

Fig 3: 2 m temperature ACC versus ERA5. a) DCPP-CTRL ACC, b) DCPP-VEG ACC, c) ACC difference, DCPP-VEG minus DCPP-CTRL. Dots represent statistically significant values, α=0.05.

Figure 4 shows the ACC difference between DCPP-VEG and DCPP-CTRL for three different variables in polar stereographic projection: a) 2m temperature (the same as Fig3c, but in polar stereographic projection), b) mean sea level pressure (MSLP) and c) the zonal wind at 850 hPa. The polar stereographic projection is best suited to highlight the large-scale features of the Northern Hemisphere, i.e., where the improved vegetation has more considerable effects. The difference in the ACC for MSLP and U850 appears to propagate from the region in central Asia, where 2m temperature improves the most, to affect a wide area to the East, including Europe and reaching the North Atlantic Ocean and Greenland. In the North American Continent, DCPP-VEG has a prediction skill improvement over Alaska, with a statistically significant reduction of the ACC values near the Hudson Bay.
Results from Fig 3c and Fig 4b,c are consistent and the MSLP and U850 improvements over the Atlantic Ocean suggests possible teleconnection pathways linked to the vegetation variability. Preliminary results indicate that the large scale effects may at least in part originate from the improved albedo variability over Asian boreal forests. The role of surface roughness variability will be also investigated in the future.

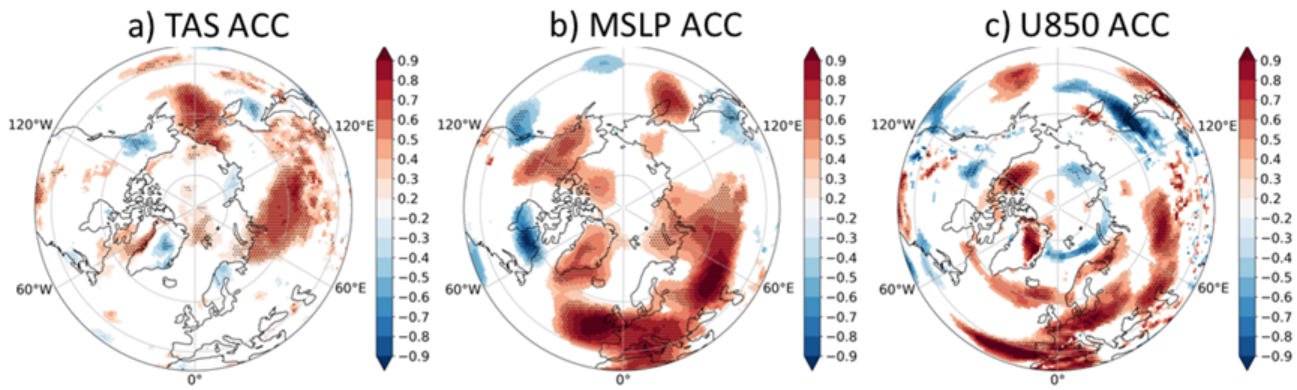

Fig 4: *ACC difference, DCPP-VEG minus DCPP-CTRL for 2 m temperature (a), mean sea level pressure (b) and zonal wind at 850 hPa (c). Dots represent statistically significant values, α=0.05.*

References:

*Balsamo, G., A. Beljaars, K. Scipal, P. Viterbo, B. van den Hurk, M. Hirschi, and A. K. Betts, 2009: A Revised Hydrology for the ECMWF Model: Verification from Field Site to Terrestrial Water Storage and Impact in the Integrated Forecast System. J. Hydrometeor., **10**, 623–643,* https://doi.org/10.1175/2008JHM1068.1.

Bilbao, R., Wild, S., Ortega, P., Acosta-Navarro, J., Arsouze, T., Bretonnière, P.-A., Caron, L.-P., Castrillo, M., Cruz-García, R., Cvijanovic, I., Doblas-Reyes, F. J., Donat, M., Dutra, E., Echevarría, P., Ho, A.-C., Loosveldt-Tomas, S., Moreno-Chamarro, E., Pérez-Zanon, N., Ramos, A., Ruprich-Robert, Y., Sicardi, V., Tourigny, E., and Vegas-Regidor, J.: Assessment of a full-field initialized decadal climate prediction system with the CMIP6 version of EC-Earth, Earth Syst. Dynam., 12, 173–196, https://doi.org/10.5194/esd-12-173-2021, 2021.

Boer, G. J., Smith, D. M., Cassou, C., Doblas-Reyes, F., Danabasoglu, G., Kirtman, B., Kushnir, Y., Kimoto, M., Meehl, G. A., Msadek, R., Mueller, W. A., Taylor, K. E., Zwiers, F., Rixen, M., Ruprich-Robert, Y., and Eade, R.: The Decadal Climate Prediction Project (DCPP) contribution to CMIP6, Geosci. Model Dev., 9, 3751–3777, https://doi.org/10.5194/gmd-9-3751-2016, 2016.

Copernicus Climate Change Service: Land cover classification gridded maps from 1992 to present derived from satellite observations, https://doi.org/10.24381/cds.006f2c9a, 2019.

Copernicus Global Land Service: Fraction of green vegetation Cover and Leaf Area Index, https://land.copernicus.eu/global/products/, last access: January 2022, 2022.https://doi.org/10.24381/cds.006f2c9a

Craig, A., Valcke, S., and Coquart, L.: Development and performance of a new version of the OASIS coupler, OASIS3-MCT_3.0, Geosci. Model Dev., 10, 3297–3308, https://doi.org/10.5194/gmd-10-3297-2017, 2017.

Dee, D.P., Uppala, S.M., Simmons, A.J., Berrisford, P., Poli, P., Kobayashi, S., Andrae, U., Balmaseda, M.A., Balsamo, G., Bauer, P., Bechtold, P., Beljaars, A.C.M., van de Berg, L., Bidlot, J., Bormann, N., Delsol, C., Dragani, R., Fuentes, M., Geer, A.J., Haimberger, L., Healy, S.B., Hersbach, H., Hólm, E.V., Isaksen, L., Kållberg, P., Köhler, M., Matricardi, M., McNally, A.P., Monge-Sanz, B.M., Morcrette, J.-.-J., Park, B.-.-K., Peubey, C., de Rosnay, P., Tavolato, C., Thépaut, J.-.-N. and Vitart, F. (2011), The ERA-Interim reanalysis: configuration and performance of the data assimilation system. Q.J.R. Meteorol. Soc., 137: 553-597. https://doi.org/10.1002/qj.828

Dorigo, W., Wagner, W., Albergel, C., Albrecht, F., Balsamo, G., Brocca, L., Chung, D., Ertl, M., Forkel, M., Gruber, A., Haas, E., D. Hamer, P., Hirschi, M., Ikonen, J., de Jeu, R., Kidd, R., Lahoz, W., Liu, Y., Miralles, D., Mistelbauer, T., Nicolai-Shaw, N., Parinussa, R., Pratola, C., Reimer, C., van der Schalie, R., Seneviratne, S., Smolander, T., Lecomte, P. ESA CCI Soil Moisture for improved Earth system understanding: State-of-the *art and future directions, Remote Sensing of Environment, Volume 203, 2017, Pages 185-215, ISSN 0034-4257, https://doi.org/10.1016/j.rse.2017.07.001.*

Döscher, R. et al.: The EC-Earth3 Earth system model for the Coupled Model Intercomparison Project 6, Geoscientific Model Development, 15, 2973–3020, https://doi.org/10.5194/gmd-15-2973-2022, 2022.

Eyring, V., Bony, S., Meehl, G. A., Senior, C. A., Stevens, B., Stouffer, R. J., and Taylor, K. E.: Overview of the Coupled Model Intercomparison Project Phase 6 (CMIP6) experimental design and organization, Geosci. Model Dev., 9, 1937–1958, https://doi.org/10.5194/gmd-9-1937-2016, 2016.
Gruber, A., Scanlon, T., Van Der Schalie, R., Wagner, W., and Dorigo, W.: Evolution of the ESA CCI Soil Moisture climate data records and their underlying merging methodology, Earth System Science Data, 11, 717–739, https://doi.org/10.5194/essd-11-717-2019, *2019*
Dorigo, W. et al.: ESA CCI Soil Moisture for improved Earth system understanding: State-of-the art and future directions, Remote Sensing of Environment, 203, 185–215, https://doi.org/10.1016/j.rse.2017.07.001, 2017
Hersbach, H, Bell, B, Berrisford, P, et al. The ERA5 global reanalysis. Q J R Meteorol Soc. 2020; 146: 1999–2049. https://doi.org/10.1002/qj.3803*https://doi.org/10.1002/qj.3803*
Hobeichi, S., Abramowitz, G., and Evans, J. P.: Robust historical evapotranspiration trends across climate regimes, Hydrol. Earth Syst. Sci., 25, 3855–3874, https://doi.org/10.5194/hess-25-3855-2021, *2021.*https://doi.org/10.5194/essd-11-717-2019https://doi.org/10.1016/j.rse.2017.07.001

Madec, G., and the NEMO team, 2008: NEMO ocean engine. Note du Pôle de modélisation, Institut Pierre-Simon Laplace (IPSL), France, No 27, ISSN No 1288-1619.

Mogensen, Kristian & Molteni, M.B.R. & Weaver, Anthony. (2012). The NEMOVAR ocean data assimilation system as implemented in the ECMWF ocean analysis system for system 4. ECMWF Tech. Memo.. 668.
https://doi.org/10.24381/cds.006f2c9a

van Oorschot, F., van der Ent, R. J., Hrachowitz, M., Di Carlo, E., Catalano, F., Boussetta, S., Balsamo, G., and Alessandri, A.: Representing inter-annual land cover and vegetation variability based on satellite observations in the HTESSEL land surface model, EGUsphere [preprint], https://doi.org/10.5194/egusphere-2023-803, 2023.

Smith, B., Wårlind, D., Arneth, A., Hickler, T., Leadley, P., Siltberg, J., and Zaehle, S.: Implications of incorporating N cycling and N limitations on primary production in an individual-based dynamic vegetation model, Biogeosciences, 11, 2027–2054, https://doi.org/10.5194/bg-11-2027-2014, 2014.